The Perugia (Italy) earthquake of April 29,1984: a seismic survey

H. Haessler, R. Gaulon, L. Rivera, R. Console, M. Frogneux, G. Gasparini, L. Martel, G. Patau, M. Siciliano, A. Cisternas

Bulletin of the Seismological Society of America, Vol. 78, No. 6, pp. 1948–1964, December 1988

THE PERUGIA (ITALY) EARTHQUAKE OF 29, APRIL 1984: A MICROEARTHQUAKE SURVEY

BY H. HAESSLER, R. GAULON, L. RIVERA, R. CONSOLE, M. FROGNEUX, G. GASPARINI, L. MARTEL, G. PATAU, M. SICILIANO, AND A. CISTERNAS

ABSTRACT

A field study after the Perugia earthquake of 29 April 1984 provided more than 300 well-recorded events concentrated within two parallel clusters separated by 2 km and trending along the Apenninic direction. The length of the aftershock area is 14 km, focal depths being shallower than 8 km. Relocation of the main event places the epicenter at the southern end of the aftershock zone, suggesting a rupture propagation from SE to NW. Most focal mechanisms are consistent with normal faulting. The spatial distribution of seismicity suggests that the Gubbio normal fault was activated during the main shock. This earthquake, together with the Norcia 1979 and the Abruzzi 1984 shocks, is typical of the extension in the high Apennines generated by the flexure of the mountain chain in response to regional compression. The Parma 1983 event, a thrust, belongs to the compression zone at the eastern flank of the chain. These results are consistent with the EW continental collision along the Apennines.

INTRODUCTION

A magnitude 5.3 (NEIC) earthquake struck the region of Perugia in Central Italy on 29 April 1984 (Lat. 43.25° N, Long. 12.52° E, depth 7 km, m_b = 5.1, M_S = 5.2; ISC). The seismic moment was 3.4 10^{24} dyne-cm (HRVD). It was widely felt, the epicentral intensity being VII to VIII. Many buildings suffered damage, 1200 were declared unsafe, 36 people were injured, and 7500 were homeless.

A French-Italian cooperation permitted the detailed study of the aftershocks of this earthquake. A similar joint field operation had already been conducted for the Norcia 1979 earthquake, situated in the same tectonic province some 70 km to the SE (Deschamps *et al.*, 1984).

Several other events accompanied the Perugia crisis: in October 1982, a seismic cluster of earthquakes with magnitude smaller than 4.5 had affected the region of Assisi, at 20 km to the SE of the Perugia main shock; in November 1983 an earthquake of magnitude 5.0 was felt in Parma at 255 km to the NW of Perugia; and finally, 1 week after the Perugia earthquake a strong event (M = 5.8) struck the Abruzzi, 200 km to the SE.

Hence, a period of intense seismic activity permitted the collection of an important amount of precise data about the seismotectonics of central Italy. Seismic information is important in this region since almost nothing (except the recent work by Westaway and Jackson, 1987) has been reported in Italy up to now, in relation to surface breaks clearly associated to earthquake faulting.

This paper is devoted to the study of the Perugia earthquake and its aftershock sequence in relation with the regional tectonics of the central Apennines.

TECTONIC SETTING

One of the main features of the tectonics of the Western Mediterranean area is the collision (Fig. 1) of the Italo-Adriatic promontory against the European continental region (Tapponnier, 1977). The Alps result from this convergence.

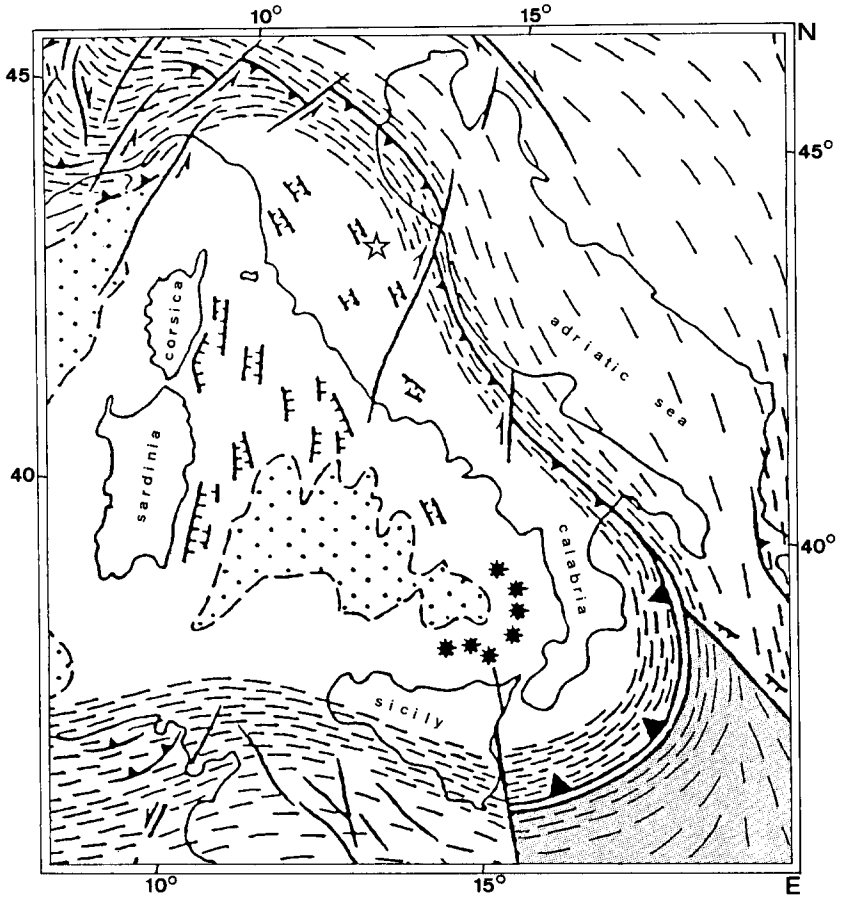

FIG. 1. Generalized tectonic map of the Tyrrhenian basin after Philip (1983). The gray region at the lower right corner is the Ionian basin. Normal faults are represented by indented lines. Dip of reverse faults is indicated by solid triangles, the larger ones corresponding to subduction. The thrust belt divides the area into two parts: the Tyrrhenian internal region to the left and the Adriatic foreland to the right. Shear faulting is shown by arrows parallel to the trace of the faults. Dotted zones are deep oceanic basins. Filled stars are active volcanoes. The open star shows the epicenter of the Perugia earthquake. The large NNE–SSW oriented fault to the south of Perugia is the Anzio-Ancona shear zone. Hatched lines correspond to compressional belts. A block diagram across Perugia is shown in Figure 3.

On the other hand, the Apennines (Fig. 1) belong to a rather different structural context where we may distinguish three main geodynamic units:

1. A collision-subduction boundary bordering the Apennines (shown by filled triangles in Figure 1), going from the SW border of the Po plain, through Ancona and the Bradonian trough, down to the Calabrian-Sicilian subduction. The present-day subduction is what remains from an ancient one that has been closed from north to south and replaced by the actual continental collision (Bousquet and Philip, 1986; Malinverno and Ryan, 1986). The thrust surface (and the plane of subduction) dips towards the Apennines. Earthquakes are crustal in northern and central Italy while intermediate and deep events are observed in the Calabrian arc (Anderson and Jackson, 1987).

2. The back-arc region, formed by the Tyrrhenian basin, Corsica, Sardinia and the western coast of Italy. This region is mainly formed by thinned continental crust (a similar situation exists in the Aegean Sea, Le Pichon and Angelier, 1979).

3. The fore-arc region, formed by the Po plain and the Adriatic basin. This

sedimentary basin is asymmetric, being deeper next to the Apennines where it reaches a thickness of 8 km (Ogniben, 1975) while thinning gently toward the east. It corresponds to the accretion prism in front of the Apennines.

The convergence is characterized by east-west tectonic shortening, by uplifting and substantial thickening of the Apenninic belt and nappe thrusting over the Adriatic foreland. Thrusting on the eastern flank of the belt is certainly active at present (Elter *et al.*, 1975).

The back-arc or internal region (the Tyrrhenian Sea and western Italy) is characterized by an extensional state of stress with $R = (\sigma_z - \sigma_x)/(\sigma_y - \sigma_x) > 1$ (R is the shape of the deviatoric stress obtained from the eigenvalues, $R > 1$ when $\sigma_z > \sigma_y > \sigma_x$, see Armijo *et al.*, 1982). There we observe normal faulting, crustal thinning, volcanism (alcaline to the north and calco-alcaline in front of the Calabrian-Sicilian arc), uplift, and positive gravity anomalies. Actually, the regional extension ceased to be active to the north of the basin, at the places where oceanic subduction stopped. Young, normal faulting occurs only at the flexure ("extrados") related to the thrust at the boundary of continental collision.

The forearc or external region (the Po plain, the Adriatic Sea and the Bradanic basin) shows compressional tectonics with $R < 0$ ($\sigma_z < \sigma_x < \sigma_y$), reverse faulting and nappes, crustal thickening, subsidence, and accretion of sediments and negative gravity anomalies.

The epicenter of the Perugia earthquake is located to the north of the back arc basin, near the transition from extensional to compressional tectonics. The relief of the Apennines is related to thrusting and flexuring of the upper crust (Philip, 1983). A simplified geological map (Fig. 2) shows a series of elongated sedimentary basins along a NNW direction. These valleys are controlled by normal faults, and are filled with Plio-quaternary deposits. We may notice, for example, the small valley at Gubbio, and the larger one that extends to the NW next to Perugia, while bifurcating towards the SE. A schematic block diagram through Perugia (Fig. 3, modified after Bousquet and Philip, 1986) illustrates the region of extension with normal faulting, the transition to compression with reverse faulting, the thickening of the crust under the Apennines, and the Adriatic sedimentary basin related to the accretion prism of the older subduction.

Field Work

The Perugia earthquake was one of a series of events that affected central Italy in recent years. Figure 4 illustrates the seismic activity from 1976 to 1985 according to the data file of the Euro-Mediterranean Seismological Center (EMSC). The clusters of seismicity correspond to the aftershocks of these earthquakes. The Parma 1983, Perugia 1984, Norcia 1979, Abruzzi 1984, and the Irpinia 1980 event to the south are clearly seen. The seismic cluster ($M < 4.5$) near Assisi in October 1982, 18 months before the Perugia event and 20 km to the south of it, is easily distinguishable too.

Two days after the main shock (see Table 1 for focal parameters) a team of seismologists from the Institutes of Physics of the Earth of Paris and Strasbourg set up a local seismic network around the epicentral area. The network, formed by 5 MEQ 800 Sprengnether analog recorders with WWV time control, and four portable 3-components digital records (GEOSTRAS) with automatic gain and DCF time signals, operated during 7 days. Several hundreds of microearthquakes ($M_L <$ 3.5) were recorded and about 300 among them, having more than five arrivals, P or S, were selected as reliable.

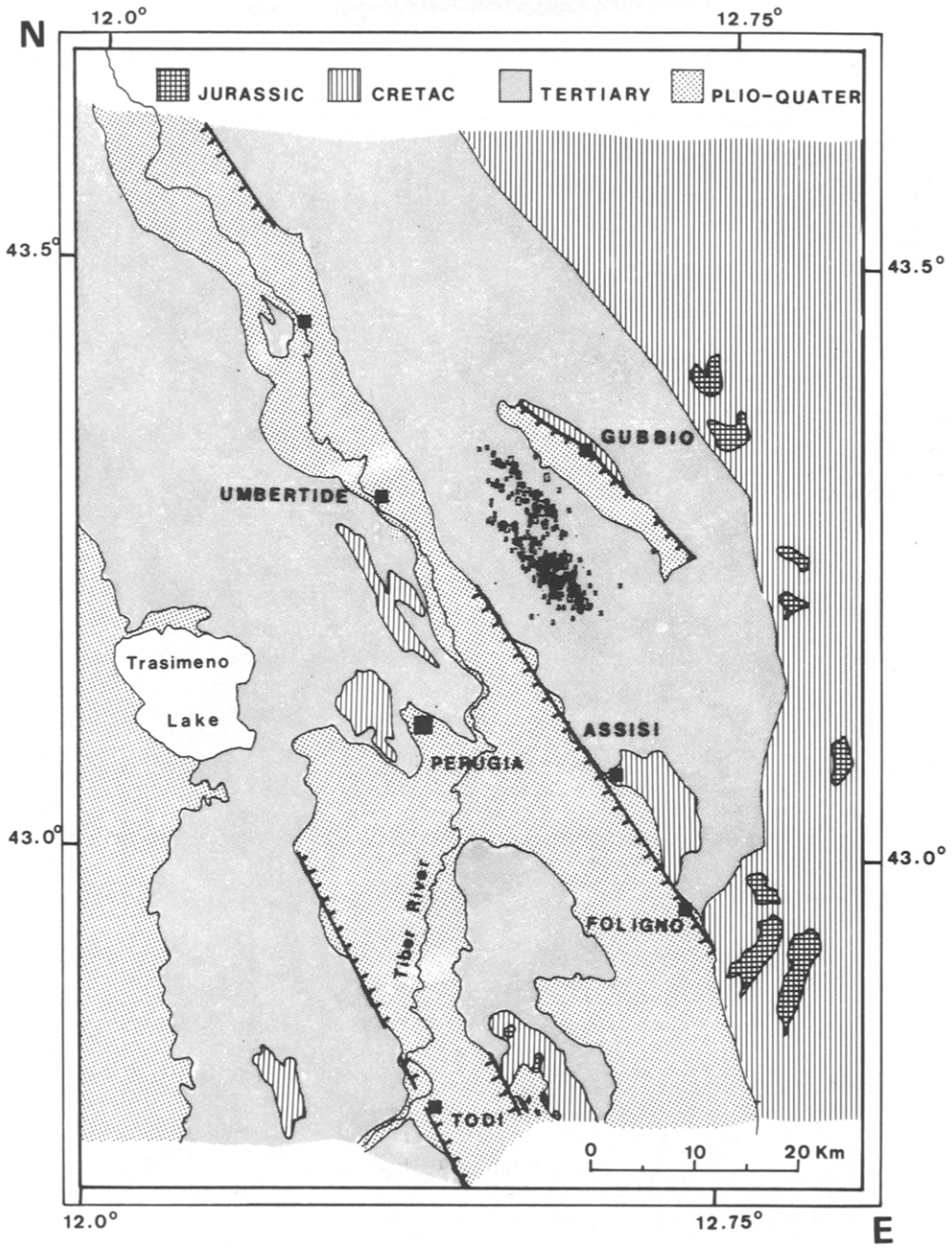

FIG. 2. Simplified geological scheme of the Perugia region displaying Plio-quaternary basins and recent faulting. Valleys are controlled by normal faulting. Aftershock clusters are located between Perugia and Gubbio and their trend is parallel to the orientation of the valleys and to the strike of the faults. Epicenters are represented by rectangles whose size increases with the magnitude.

We computed hypocentral determinations by using the velocity model of Deschamps *et al.* (1984) for the 1979 Norcia earthquake and the HYPO71 routine. The ratio $Vp/Vs = 1.85$ was established from a composite Wadati diagram. A simpler model consisting of a homogeneous half-space with a velocity of 5.5 km/sec does

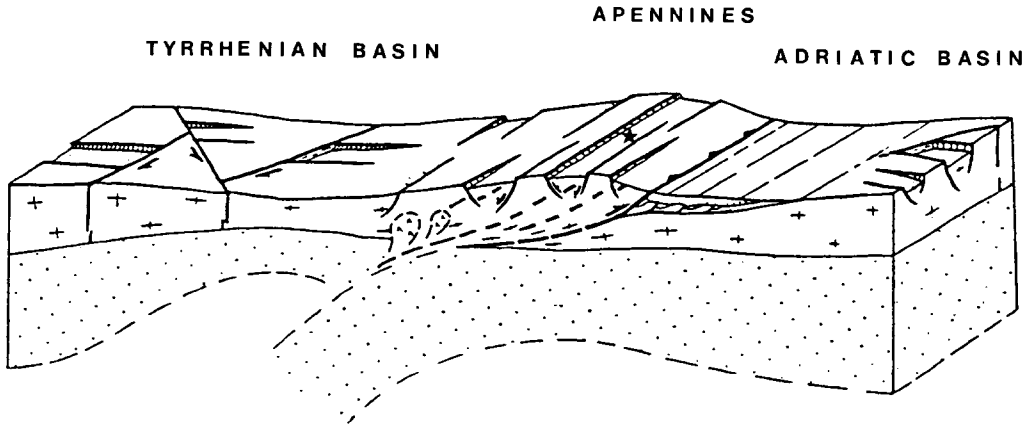

FIG. 3. Schematic block diagram across Perugia showing continental subduction (after Bousquet and Philip, 1986). Crosses correspond to crustal material and dots to the lithospheric mantle. The Moho level shows crustal thickening at the collision front. On the contrary, the crust is thinner where extension took place. An accretion prism is observed in the Adriatic basin. The star shows the relative position of the Perugia earthquake.

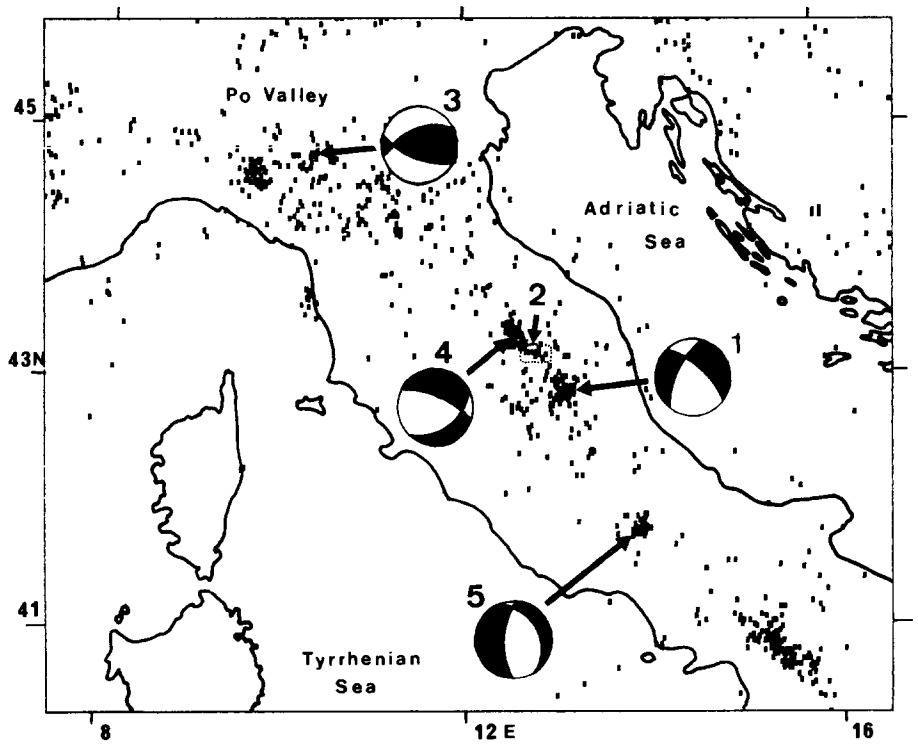

FIG. 4. Recent seismicity of central Italy (1976–1985). Data from the Euro-Mediterranean Seismological Center (EMSC). The focal mechanisms are those of Figure 7. 1. Norcia 1979. 2. Assisi sequence of 1982. 3. Parma 1983. 4. Perugia 1984. 5. Abruzzi 1984.

not considerably change the distribution of epicenters. The frequency distribution of the standard errors of horizontal and vertical focal coordinates (Fig. 5 a, b) shows accuracies of the order of 0.5 and 1.0 km, respectively. The magnitude was obtained from the coda length t_c of the MEQ-800 records through the following formula: $M = 2.5 \log t_c - 1.9$.

TABLE 1

ISC PARAMETERS

Event	Date Origin Time	Latitude	Longitude	Depth	*Mb*	*Ms*	Seismic Moment
NORCIA	19-09-1979 21:35:36.8	42.80 N	13.04 E	6 km	5.8	5.9	0.7 10^{25}dyne-cm (Deschamps)
PARMA	9-11-1983 16:29:51.8	44.68 N	10.28 E	38 km	4.9	4.9	
PERUGIA	29-04-1984 5:02:59.3	43.25 N	12.52 E	7 km	5.1	5.2	3.4 10^{24}dyne-cm (HRVD)
ABRUZZI	7-05-1984 17:49:42.7	41.76 N	13.90 E	16 km	5.4	5.8	7.8 10^{24}dyne-cm (HRVD)

Note: all data except Seismic Moment are from ISC Bulletins. The depth of the Parma earthquake is based on both pP-P delays and the normal hypocenter determination.

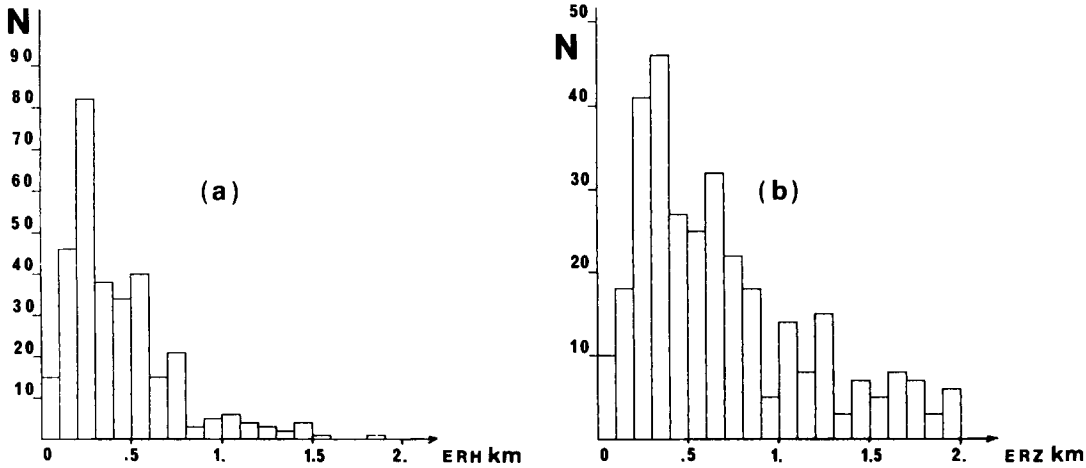

FIG. 5. a) Frequency distribution of the standard errors ERH = $(ERX^2 + ERY^2)^{.5}$ of the epicenters in km . ERX and ERY are the standard errors in the EW and NS directions respectively. 80 per cent of the ERHs are less than .5 km. b) Frequency distribution of the standard errors ERZ of the focal depths in km. 80 per cent of ERZ are less than 1 km.

The spatial distribution of aftershocks and the location of the seismic stations are shown in Figure 6. The epicenters follow a N140E direction and lie within a domain of about 20 km long and 6 km wide. They show a remarkable agreement with the direction of the major tectonic features of the region (Fig. 2). The same orientation was also obtained in the case of the Norcia earthquake (Deschamps *et al.*, 1984). The epicentral distribution seems to follow two parallel linear clusters, the denser one being to the southwest. It is interesting to observe that the aftershocks lie in between the valleys of Gubbio and Perugia. As we have mentioned, these valleys are formed by normal faulting and filled with Quaternary sediments. The Gubbio valley is an elongated basin, limited to the east by a fault scarp, 20 km long, dipping to the west. Since no surface rupture was observed, it is not certain that this is the fault responsible for the earthquake. Nevertheless, the geometrical distribution of aftershocks suggests that either its prolongation in depth or an equivalent en-echelon fault system are involved (see Figs. 2 and 7c). A cross-section along the strike of the clusters (Fig. 7b) shows that the depth of aftershocks is smaller than 8 km, namely they are shallower than those of the Norcia sequence (h

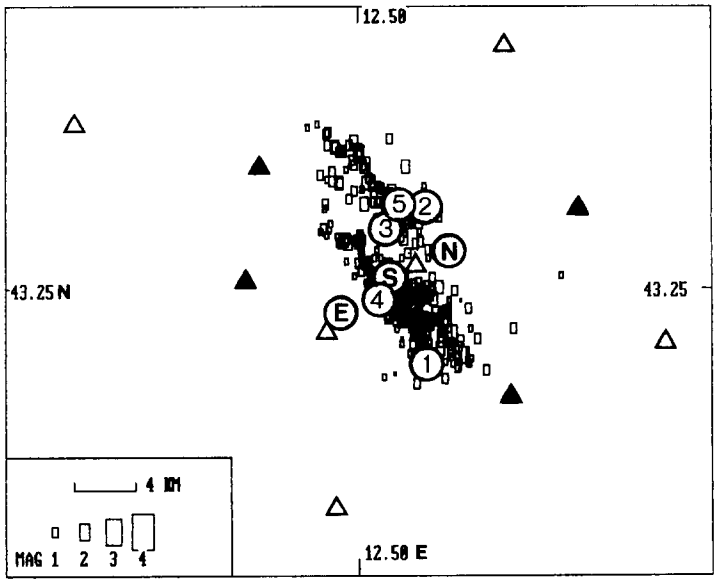

FIG. 6. Epicenters of aftershocks (rectangles) recorded from 6 May to 10 May 1984. Open circles with numbers are: the main shock (1), and the aftershocks (2), (3) and (4), of magnitude higher than 4 relocated using the 10 May 1984, 9:45 hrs shock ($M = 4.0$) as master event (5). Open circles with letters are main shock locations given by the international agencies, E: EMSC, N: NEIC, S: ISC. Open triangles are the MEQ stations and filled triangles are the GEOSTRAS digital stations. The aftershocks are distributed along two parallel clusters striking NW.

< 15 km) (Deschamps *et al.*, 1984). The cross section in the direction NE–SW (Fig. 7c) shows a separation of about 2 km between the clusters.

FOCAL MECHANISM AND RELATED EARTHQUAKES

The focal mechanism of the Perugia earthquake is presented in Figure 8, together with those of the Norcia (September 19, 1979, $M_S = 5.9$), Abruzzi (May 7, 1984, $M_S = 5.8$) and Parma (November 9, 1983, $M_S = 4.9$) earthquakes.

The Norcia mechanism, determined by Deschamps *et al.* (1984) from the analysis of long period *P*-wave forms (Fig. 8a), showed a normal fault with an important right lateral shear component. The others (Figs. 8b, c, d) were obtained by us on the basis of ISC bulletin readings of the initial motion of short- and long-period body waves. We adopted the following selection criteria: a reading was acceptable either if it was from a short-period wave closer than 10° to the epicenter, or from a long-period, pure-mantle-path, direct *P* wave observation. The maximum likelihood algorithm of Brillinger *et al.* (1980) was used in order to obtain the best nodal solution in each case.

The Perugia event, with a WNW strike, has a small left lateral shear component (Fig. 8c). An independent calculation, the HARVARD solution (Fig. 8e) from long-period surface waves inversion, gives an almost pure normal fault, one of the planes being parallel to the Apenninic direction as in our mechanism.

The Abruzzi mechanism (Fig. 8d, f) also shows normal faulting with one nodal plane oriented along the Apenninic direction. We observe here a small clockwise rotation of the axis of the chain and of the azimuth of the fault plane, with respect to Perugia.

The Parma mechanism (Fig. 8b) represents a reverse fault almost without shear

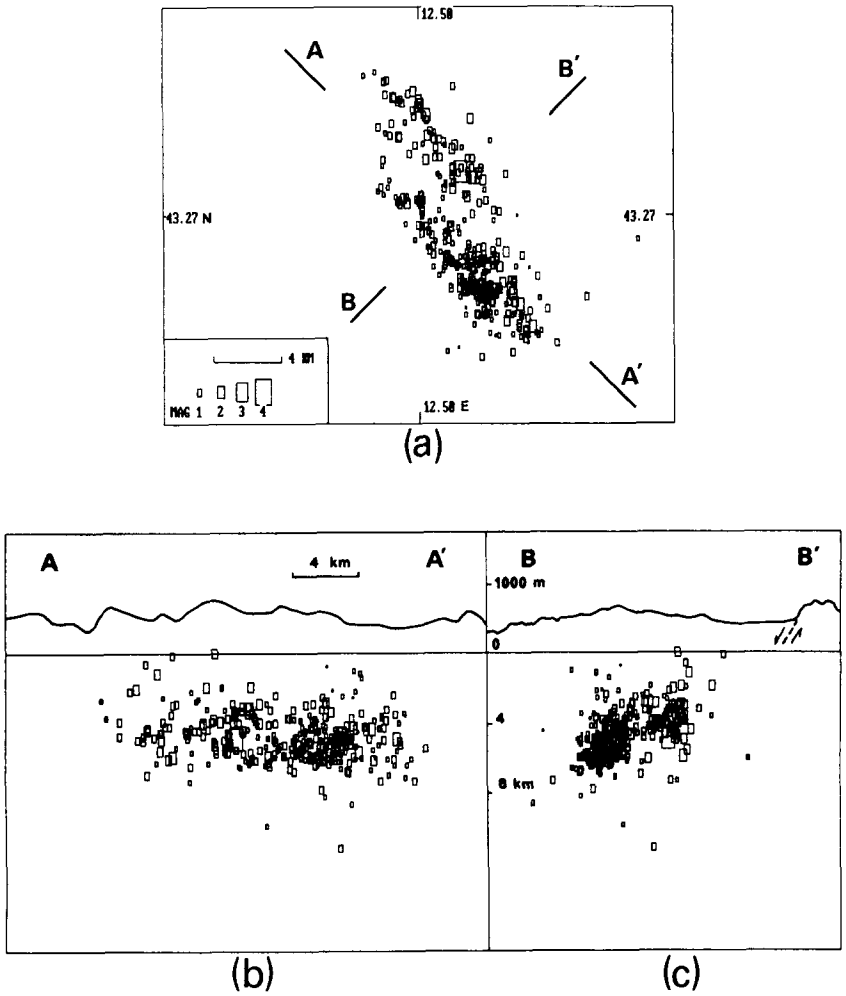

FIG. 7. a) Epicenter distribution showing the orientation of the cross sections. b) Cross section along the strike of the clusters of aftershocks. Depth is smaller than 8 km in general. c) Cross section orthogonal to the strike of aftershocks. Two independent clusters are separated by 2 km. The topographic scale is exaggerated four times and the surface trace of the Gubbio normal fault plane is shown.

and therefore differs from that of the other three shocks. This mechanism shows that this event is within the compression region, and indeed its epicenter and its strike correspond well to the Apenninic thrust. Hence it is likely that the fault plane is that pointing to the southwest.

Stress-compatible focal mechanisms of 65 aftershocks (Table 2) of the Perugia earthquake are shown in Figure 9a, b, c, d. In our case, we have five or more polarities for each event. Evidently, individual solutions cannot be obtained by the usual methods. Therefore, we need to make some assumptions in order to deal with the total number of earthquakes in a collective way. The hypothesis is that the same regional stress tensor acts on each fault plane. The stress tensor (more exactly, its orientation and shape) and the different fault planes are jointly estimated, by a maximum likelihood procedure (Rivera and Cisternas, Submitted for publication). The method permits, in general, the discrimination of the fault plane from the auxiliary plane under the assumption of a single stress tensor acting on the faults.

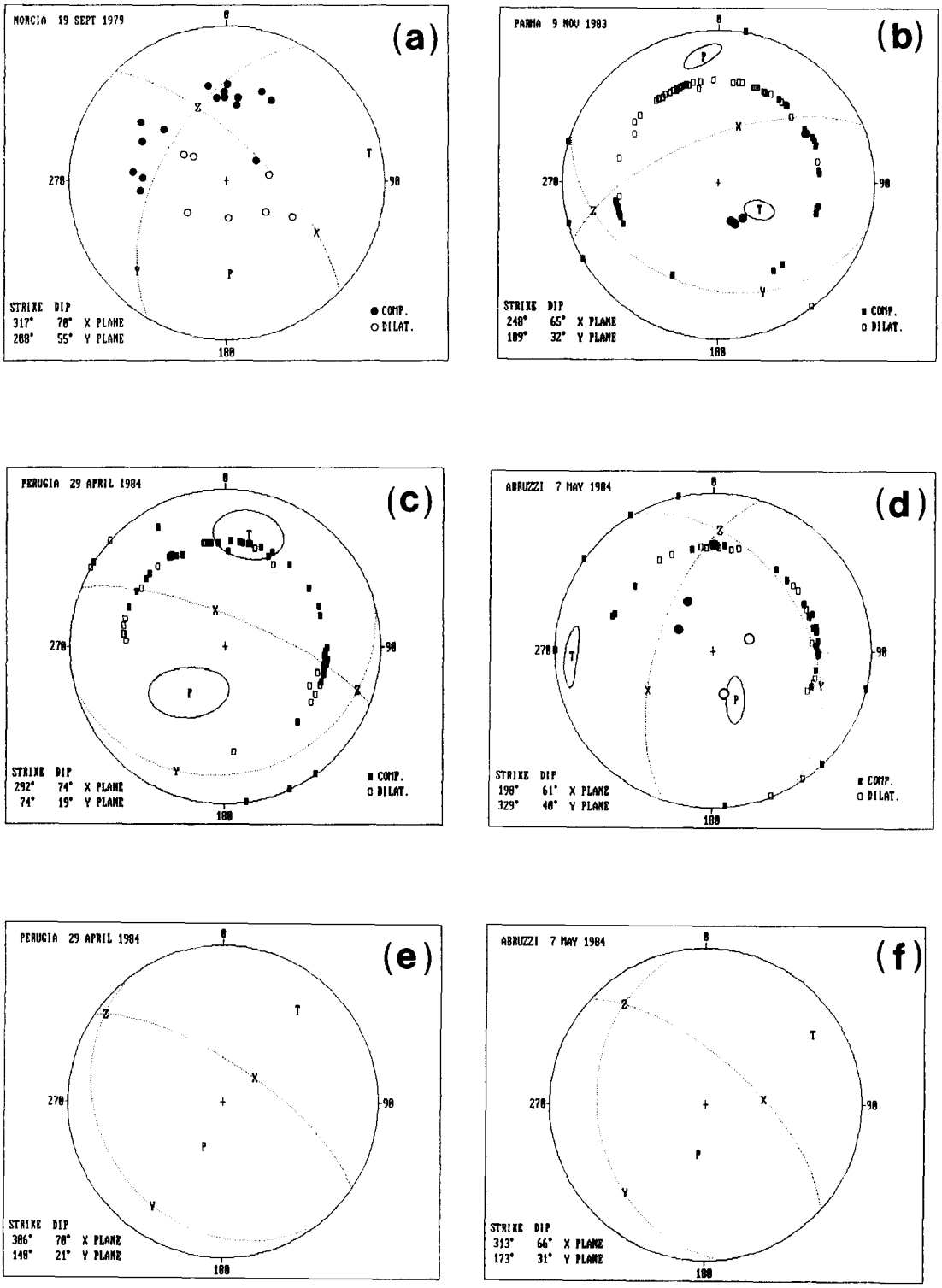

FIG. 8. Focal mechanism of recent Italian earthquakes. Schmidt lower hemisphere projection. Compression readings on short- and long-period records are shown as filled squares and circles, respectively. The Norcia (a) mechanism is taken from Deschamps *et al.* (1984). The Parma (b), Perugia (c) and Abruzzi (d) mechanisms were obtained from first motion body wave readings (short and long period) by using the maximum likelihood algorithm of Brillinger *et al.* (1980). Confidence regions for *P* and *T* axes correspond to one standard deviation. The Parma shock is the only one showing a reverse fault. The Perugia (e) and Abruzzi (f) nodal solutions determined by Harvard on a routine basis (NEIC, monthly listing), using a long-period body and mantle wave tensor inversion.

TABLE 2

LIST OF PERUGIA AFTERSHOCKS WITH FOCAL MECHANISM (FIGURE 9a, b, c, d)

N	Date			Origin Time			Latitude		Longitude		Depth	ERZ	MAG	RMS	ERX	ERY
	y	m	d	h	m	sec.	°N	min.	°E	min.	km	km		sec	km	km
1	84	05	05	10	23	4.63	43	13.78	12	33.04	4.53	0.7	1.4	0.04	0.3	0.2
2	84	05	05	10	44	31.67	43	15.82	12	31.41	6.01	0.7	1.7	0.04	0.4	0.4
3	84	05	05	10	46	57.09	43	13.72	12	33.25	5.07	0.3	0.9	0.02	0.2	0.1
4	84	05	05	12	16	10.26	43	15.01	12	33.84	2.88	1.0	1.5	0.06	0.3	0.3
5	84	05	05	20	7	32.17	43	16.67	12	29.95	5.68	0.2	1.0	0.02	0.1	0.1
6	84	05	05	20	20	47.48	43	13.76	12	33.13	4.77	0.6	1.1	0.08	0.3	0.4
7	84	05	05	20	44	13.81	43	19.30	12	30.23	3.62	1.0	1.2	0.06	0.2	0.3
8	84	05	05	21	52	31.36	43	12.68	12	35.03	4.96	0.7	2.1	0.10	0.4	0.5
9	84	05	05	22	9	14.54	43	18.66	12	30.37	4.64	0.3	1.7	0.04	0.2	0.2
10	84	05	05	22	29	23.63	43	14.68	12	32.79	4.92	0.3	0.9	0.04	0.2	0.2
11	84	05	05	22	46	38.90	43	19.30	12	30.33	6.05	1.4	2.0	0.08	0.4	0.5
12	84	05	05	23	0	59.90	43	19.81	12	29.22	5.13	0.4	1.4	0.04	0.2	0.2
13	84	05	05	23	4	30.45	43	14.71	12	32.16	6.20	0.5	0.8	0.04	0.2	0.2
14	84	05	06	1	4	46.04	43	16.55	12	29.51	3.98	0.8	1.5	0.08	0.2	0.2
15	84	05	06	1	9	22.48	43	14.64	12	32.13	5.43	0.4	1.0	0.02	0.1	0.2
16	84	05	06	2	23	37.67	43	16.66	12	30.00	5.90	0.2	0.8	0.02	0.1	0.1
17	84	05	06	3	59	53.35	43	14.28	12	35.26	4.28	0.7	1.1	0.04	0.1	0.2
18	84	05	06	4	32	18.54	43	13.85	12	32.16	6.35	0.6	1.2	0.04	0.2	0.2
19	84	05	06	4	49	15.78	43	16.76	12	30.11	5.54	0.1	1.1	0.00	0.0	0.0
20	84	05	06	6	41	38.09	43	14.00	12	32.41	6.01	0.3	1.1	0.02	0.1	0.1
21	84	05	06	7	4	50.72	43	13.86	12	32.66	4.96	0.8	1.6	0.08	0.5	0.5
22	84	05	06	10	58	24.81	43	13.85	12	32.96	6.15	0.6	2.0	0.04	0.2	0.2
23	84	05	06	11	12	8.47	43	13.94	12	33.62	4.97	0.9	1.0	0.12	0.9	0.7
24	84	05	06	12	11	57.77	43	18.37	12	31.58	3.84	1.0	1.8	0.05	0.3	0.2
25	84	05	06	12	29	6.05	43	18.94	12	28.23	7.11	1.0	1.2	0.05	0.3	0.3
26	84	05	06	15	10	22.87	43	14.65	12	32.57	6.13	0.2	1.2	0.02	0.1	0.1
27	84	05	06	15	45	48.45	43	13.46	12	34.26	4.52	0.7	1.6	0.05	0.2	0.3
28	84	05	06	16	29	19.57	43	13.87	12	32.77	5.47	0.3	1.1	0.02	0.1	0.1
29	84	05	06	20	5	42.82	43	14.86	12	33.45	2.58	0.1	1.1	0.00	0.0	0.0
30	84	05	06	20	28	27.90	43	14.13	12	34.20	4.75	0.6	1.6	0.05	0.2	0.3
31	84	05	06	21	27	57.46	43	13.10	12	33.94	5.02	0.3	1.1	0.02	0.2	0.1
32	84	05	06	21	29	14.51	43	17.65	12	31.49	4.70	0.2	1.6	0.03	0.2	0.1
33	84	05	06	23	52	58.41	43	14.58	12	33.57	3.42	0.8	1.5	0.04	0.2	0.3
34	84	05	07	0	51	11.77	43	13.32	12	33.04	5.37	0.6	1.3	0.06	0.2	0.2
35	84	05	07	1	33	47.03	43	16.26	12	33.56	3.31	0.4	0.9	0.04	0.2	0.2
36	84	05	07	2	7	44.74	43	14.28	12	32.85	5.42	0.5	1.0	0.03	0.2	0.2
37	84	05	07	2	28	47.41	43	14.03	12	32.33	6.25	0.4	1.1	0.02	0.2	0.1
38	84	05	07	4	16	53.15	43	13.82	12	32.41	5.80	0.8	1.3	0.05	0.3	0.3
39	84	05	07	4	24	55.21	43	17.04	12	28.34	6.62	0.4	1.1	0.04	0.2	0.3
40	84	05	07	16	23	20.92	43	12.29	12	34.71	5.35	1.2	1.4	0.04	0.3	0.2
41	84	05	07	18	28	55.20	43	13.06	12	34.30	4.82	1.6	1.5	0.11	0.7	0.7
42	84	05	07	19	28	9.13	43	13.99	12	33.15	5.71	0.7	1.3	0.04	0.3	0.3
43	84	05	07	22	51	23.66	43	17.31	12	32.23	3.58	0.4	1.1	0.04	0.2	0.2
44	84	05	07	22	52	25.60	43	13.92	12	33.52	4.59	0.6	0.9	0.05	0.2	0.2
45	84	05	07	23	59	8.06	43	15.17	12	32.85	3.02	0.6	1.4	0.06	0.3	0.3
46	84	05	08	2	23	20.21	43	13.75	12	34.15	5.75	0.6	2.0	0.02	0.2	0.2
47	84	05	08	4	26	4.19	43	18.62	12	29.11	6.16	0.5	1.7	0.04	0.4	0.3
48	84	05	08	11	21	59.10	43	15.55	12	30.56	5.65	0.3	1.0	0.02	0.3	0.2
49	84	05	08	12	25	10.67	43	13.16	12	34.89	5.07	2.3	1.1	0.06	0.6	0.6
50	84	05	08	15	11	34.35	43	13.06	12	34.12	5.62	1.7	0.6	0.07	0.4	0.5
51	84	05	08	15	31	44.43	43	13.05	12	34.50	4.36	1.4	0.8	0.04	0.3	0.3
52	84	05	08	16	22	59.00	43	13.79	12	31.99	5.15	0.2	0.7	0.02	0.1	0.1
53	84	05	08	18	17	39.31	43	17.26	12	32.85	4.09	0.4	1.5	0.03	0.3	0.2

TABLE 2—(*continued*)

N	Date			Origin Time			Latitude		Longitude		Depth	ERZ	MAG	RMS	ERX	ERY
	y	m	d	h	m	sec.	°N	min.	°E	min.	km	km		sec	km	km
54	84	05	08	18	20	8.59	43	13.79	12	32.82	5.65	0.9	1.1	0.08	0.4	0.4
55	84	05	08	18	23	40.33	43	13.72	12	33.08	4.81	0.3	0.7	0.05	0.2	0.2
56	84	05	08	18	48	27.67	43	13.83	12	32.85	4.98	0.4	1.4	0.04	0.3	0.2
57	84	05	08	18	49	18.62	43	13.73	12	33.15	4.89	0.2	1.5	0.04	0.1	0.1
58	84	05	08	21	4	4.06	43	15.26	12	32.18	5.86	0.5	1.0	0.04	0.3	0.2
59	84	05	09	2	37	44.47	43	14.55	12	31.69	5.47	0.4	0.7	0.06	0.3	0.3
60	84	05	09	2	38	50.87	43	14.63	12	31.65	5.24	0.4	1.1	0.05	0.3	0.3
61	84	05	10	0	50	58.47	43	17.35	12	32.36	3.26	0.2	2.0	0.01	0.2	0.1
62	84	05	10	2	10	17.70	43	17.43	12	31.47	4.10	0.3	1.1	0.03	0.2	0.2
63	84	05	10	5	2	8.91	43	14.92	12	31.17	5.97	0.7	1.4	0.08	0.5	0.4
64	84	05	10	5	51	58.42	43	16.58	12	30.14	4.78	0.3	0.9	0.03	0.4	0.2
65	84	05	10	9	5	3.41	43	14.69	12	31.47	6.88	0.7	1.2	0.10	0.5	0.4

At the same time, it is possible to estimate confidence ellipses around the poles of the fault planes. Even in the case when each individual shock has few polarities, the total data set may still enable us to constrain the parameters of the stress tensor.

The stress tensor (Fig. 10) depends on the polarity data set as a whole. It has the σ_1 axis almost vertical, the σ_2 axis trending in an EW direction and the σ_3 axis with a NS orientation. Confidence regions correspond to one standard deviation: the σ_3 axis is better constrained than σ_1 or σ_2, and these are better determined in the NS than in the EW direction. The shape factor R is equal to 1.1, corresponding almost to a uniaxial extension (Armijo *et al.*, 1982).

The slip direction (Fig. 9a, b, c, d) is not discriminated in this case because of the ambiguity inherent to an almost axially symmetric tensor. At the same time, fault and auxiliary planes cannot be distinguished. Error ellipses are shown for the pole of one of them, except when errors are too large and the mechanism is not well constrained (dotted lines). Normal faulting dominates in most of the solutions and 94 per cent of the observed polarities are correctly predicted by the model. This stress state is also compatible with the mechanism of the main earthquake.

Discussion and Conclusions

The analysis of the data from recent seismic events recorded in central Italy shows a remarkable agreement between the fault mechanisms and the mechanical models deduced from neotectonic information (Bousquet and Philip, 1986). The region of the Perugia (1984), Parma (1983), Norcia (1979), and Abruzzi (1984) earthquakes is situated at the north-eastern border of the Tyrrhenean basin, where continental collision takes place. We observe that thrusts occur very close to normal faults, and that the strike of both is parallel to the main Apenninic direction. Reverse faulting is present at the eastern flank of the mountains (Parma) while normal faulting dominates around the axis of the chain (Perugia, Norcia, Abruzzi). This situation is not unusual in tectonics; for instance, the El Asnam 1980 earthquake showed normal faulting next to the main thrust that was interpreted as being due to an "extrados" flexure on the hanging wall (Cisternas *et al.*, 1982). Bousquet

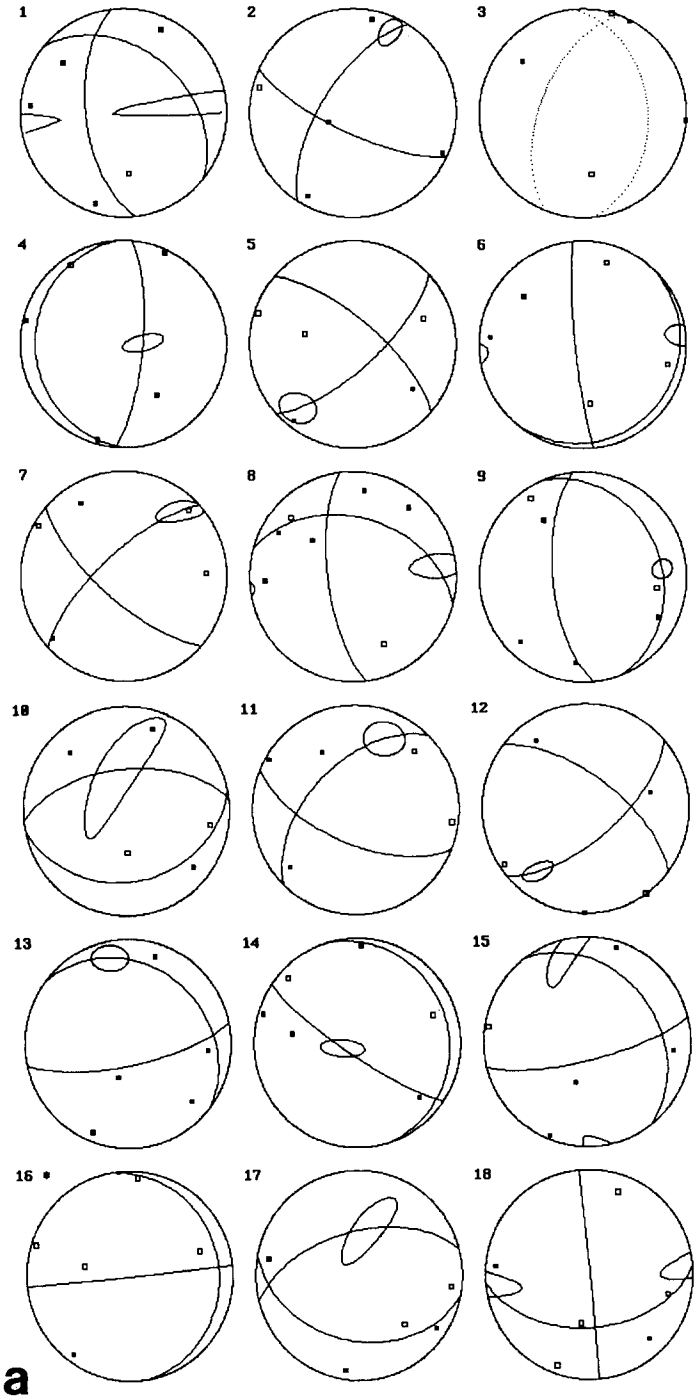

FIG. 9 a,b,c,d. Stress-compatible focal mechanisms of 65 well-recorded aftershocks of the Perugia sequence. Schmidt lower hemisphere projection. The one standard error ellipses correspond to the pole of one of the nodal planes, and they are not shown if the uncertainty is too large. In the latter case the nodal planes are drawn in dotted lines.

and Philip (1986) extended this model to a larger scale in order to explain the tectonics of the Apennines. Other cases of extensional tectonics in mountain countries may be found in Tibet and the high Andes (Armijo *et al.*, 1986; Carey-Gailhardis and Mercier, 1987). Nevertheless, the elevation, the areas involved, and

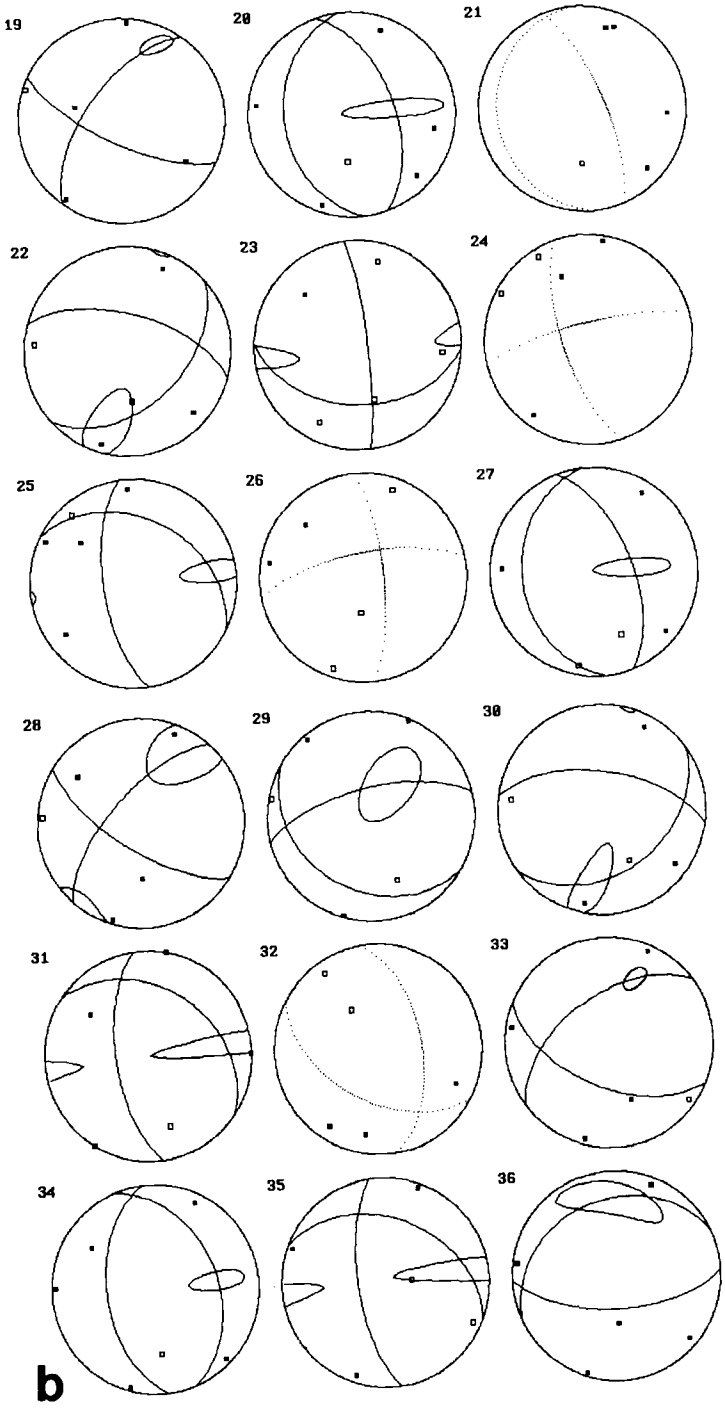

the velocity of the convergence are more important, and the tectonics more complex, than in the Apennines. One important exception to the simple cylindrical model of an "extrados" flexure next to a thrust is the right lateral Anzio-Ancona shear zone, but no well-determined focal mechanism has been obtained on this fault.

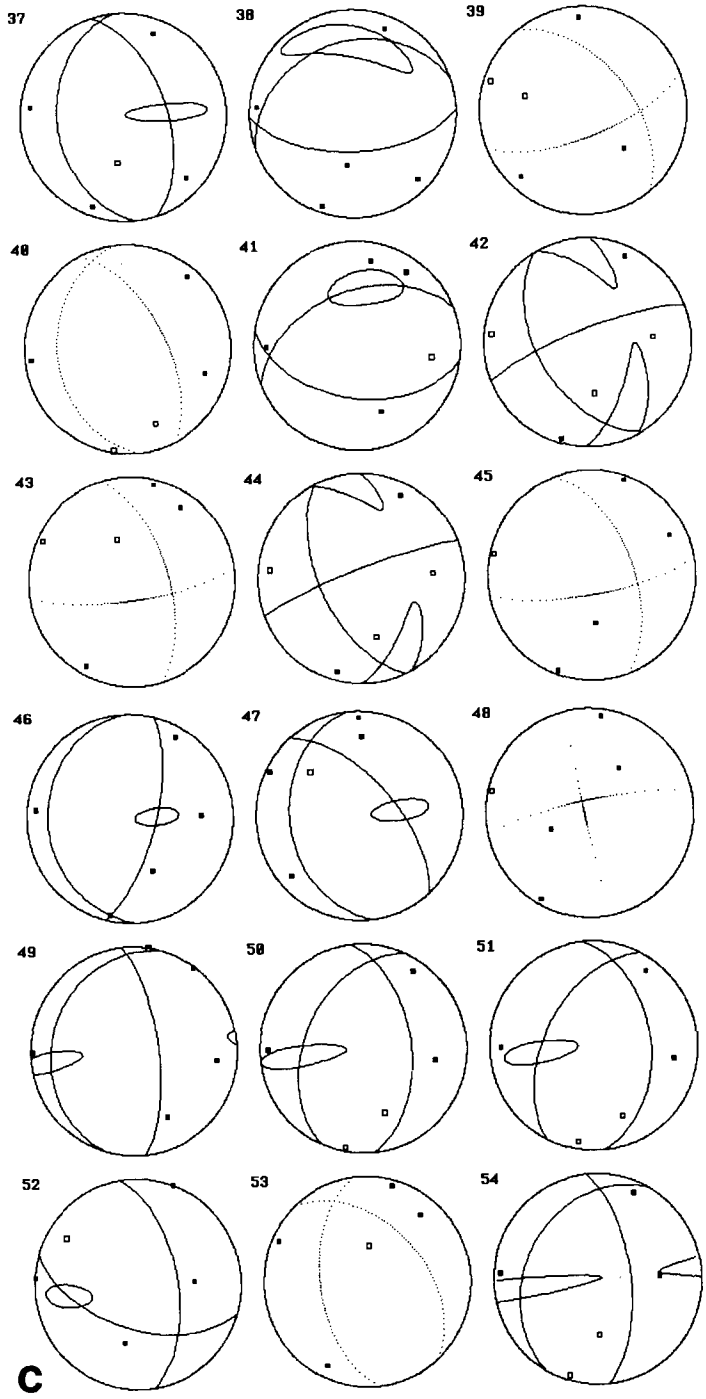

The focal mechanism of the Perugia main shock corresponds to a normal fault with a small left-lateral strike-slip component. On the other hand, the Norcia mechanism was that of a normal fault with an important right-lateral shear component. The difference could be attributed to the change in direction of the axis of the Apennines when passing from Perugia to Norcia.

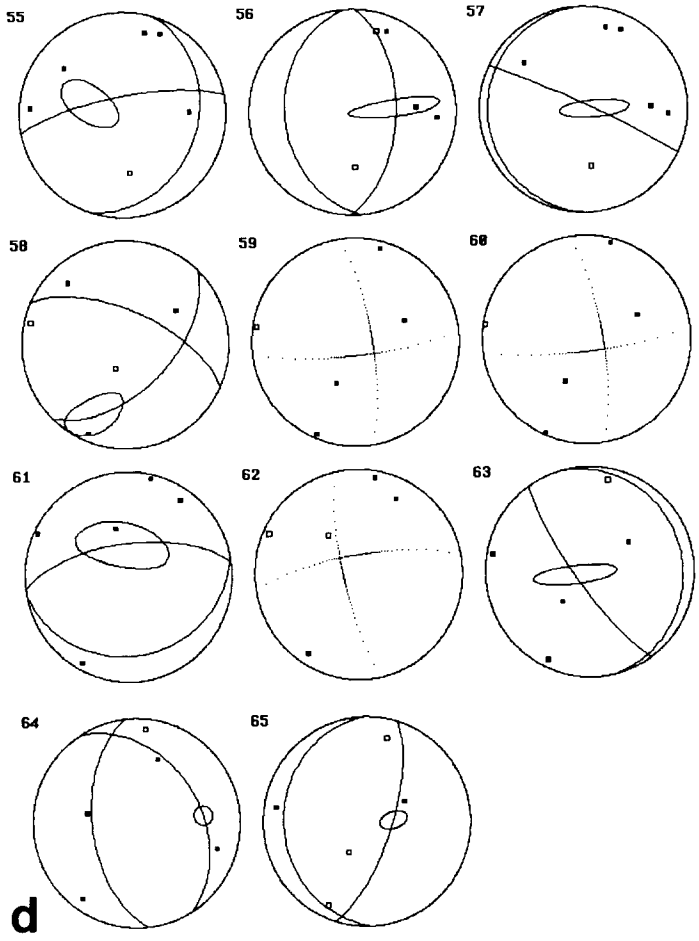

The precision obtained by using a local network displayed over the hypocentral region allows us to map in detail the structure of the ruptured zone. In the case of the Perugia aftershocks, we obtained a distribution into two clusters, each one having an elongated shape parallel to the Apenninic direction with individual depths ranging from 2 to 8 km. The orientation of the clusters provides sufficient evidence to select the fault plane in the mechanism of the main shock. Moreover, the epicenter of the main shock is located at the SE edge of the large cluster, hence showing a rupture that propagated toward the NW. The application of the method of Rivera and Cisternas (submitted for publication) to obtain stress-consistent focal mechanisms to the Perugia aftershocks shows that they are compatible with an almost uniaxial extensional state of stress with the σ_3 axis oriented NS. This confirms the stress regime inferred from the main shock.

The orientations of the stresses are in agreement with the overall tectonic scheme already presented, but absolute values of seismic deformations are at odds with those inferred from tectonics. According to Malinverno and Ryan (1986), the Apennines show a shortening of about 200 to 320 km since some 12 m.y. B.P. These values give an average rate of shortening of 1.6 to 2.6 cm/yr. These numbers are one order of magnitude higher of what may be estimated from earthquake associated deformation during this century (1 to 4 mm/yr; Anderson, 1987; Jackson and

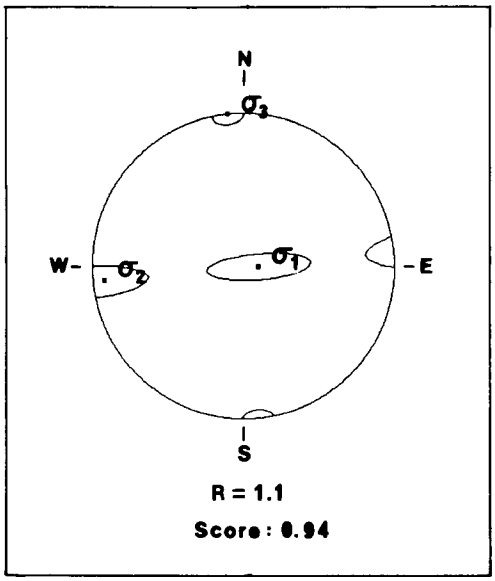

FIG. 10. Stress tensor orientation and shape factor R, for the Perugia 1984 aftershock sequence. Lower hemisphere Schmidt projection. The stress correspond to almost uniaxial extension with a NS oriented σ_3 axis. Confidence regions correspond to one standard deviation. The score is the percentage of consistent polarities.

McKenzie, 1988). Furthermore, strong earthquakes during the last decades seem to be more related to normal faulting in the high Apennines than to thrusts on the eastern flank of the chain. Since thrust should be the main mechanism for shortening, it is likely that aseismic deformation is responsible for most of the effect. It is also possible that recurrence times for large earthquakes associated to thrust are longer than some centuries. In that case, the record would not be complete and large thrust events could occur in the future.

Thus, normal faulting appears to be the most seismogenic feature in the Apennines. Nevertheless, a problem that puzzled seismologists for years in this region was the absence of surface faulting directly related to earthquakes in the Apennines, in spite of the fact that geologists had abundant mapping of Quaternary active faulting (Bousquet and Philip, 1986). This question seems to be partially answered by the recent mapping of the surface breaks corresponding to the Irpinia earthquake (Westaway and Jackson, 1987).

ACKNOWLEDGMENTS

The field work was financed by the ATP Sismogenèse de l'Institut National des Sciences de l'Univers (France). We are grateful to Michel Cara for his encouragement and help in preparing the expedition. Hervé Philip made several important tectonic suggestions and kindly allowed us to use Figures 1 and 3. M. Ferretti of Perugia gave us valuable advice. A Cisternas and L. Rivera are associated with the "Centro de Estudios Científicos de Santiago."

REFERENCES

Anderson, H. (1987). Is the Adriatic an African promontory? *Geology* **15,** 212–215.

Anderson, H. and J. Jackson (1987). The deep seismicity of the Tyrrhenian sea, *Geophys. J. R. Astr. Soc.* **91,** 613–637.

Armijo, R., E. Carey, and A. Cisternas (1982). The inverse problem in microtectonics and the separation of tectonics phases, *Tectonophysics* **92,** 145–160.

Armijo, R., P. Tapponnier, J. L. Mercier, and T.-L. Han (1986). Quaternary extension in southern Tibet: field observations and tectonic implications, *J. Geophys. Res.* **91,** B14, 13803–13872.

Bousquet, J. C. and H. Philip (1986). Neotectonics of the Calabrian arc and Apennines (Italy): an example of plio-quaternary evolution from island arcs to collisional stages, in *The Origin of Arcs.* F. C. Wezel, Editor, Elsevier Sc. Publishers, Amsterdam, 305–3326.

Brillinger, D. R., A. Udias, and B. A. Bolt (1980). A probability model for regional focal mechanism solutions, *Bull. Seism. Soc. Am.* **70,** 149–170.

Carey-Gailhardis, E. and J. L. Mercier (1987). A numerical method for determining the state of stress using focal mechanisms of earthquake populations: application to Tibetan teleseisms and microseismicity of southern Peru, Earth Planet. *Sci. Lett.* **82,** 165–179.

Cisternas, A., J. Dorel, and R. Gaulon (1982). Models of the complex source of El Asnam earthquake, *Bull. Seism. Soc. Am.* **72,** 2245–2266.

Deschamps, A., G. Iannaccone, and R. Scarpa (1984). The Umbrian earthquake (Italy) of 19 September 1979, *Ann. Geophys.* **2,**, 29–36.

Elter, P., G. Giglia, M. Tongiorgi, and L. Trevisan (1975). Tensional and compressional areas in the recent (Tortonian and present) evolution of the northern Apennines, *Boll. di Geofisica Teoretica e Applicata.* **XVII,** 65, 3–18.

Horvath, F. and H. Berckhemer (1982). Mediterranean backarc basins, in *Alpine Mediterranean Geodynamics,* H. Berckhemer and K. Hsu, Editors, Geodynamics Series, vol. 7. American Geophysical Union, Washington, D.C.

Jackson, J. A. and D. P. McKenzie (1988). The relationship between plate motions and seismic moment tensors, and the rate of active deformation in the Mediterranean and Middle East, *Geophys. J.* **93,** 45–73.

Le Pichon, X. and J. Angelier (1979). The Hellenic Arc and Trench System: A key to the Neotectonic evolution of eastern Mediterranean area, *Tectonophysics* **60,** 1–42.

Malinverno, A. and W. B. F. Ryan (1986). Extension in the Tyrrhenian sea and shortening of the Apennines as result of arc migration driven by sinking of the lithosphere, *Tectonics* **5,** 2, 227–246.

Ogniben, L. (Editor) (1975). *Structural Model of Italy. Scale 1:1.000.000,* Consiglio Nazionale delle Ricerche.

Philip, H. (1983). Le tectonique actuelle et récente dans le domaine Méditerraneen et ses bordures, ses relations avec la sismicité, *Ph.D. Thesis,* University of Science and Techniques of Languedoc, Montpellier.

Tapponnier, P. (1977). Evolution tectonique du système alpin en Méditerranée: poinçonnement et écrasement rigide-plastique, *Bull. Soc. Geol. Fr.* **19,** 437–460.

Westaway, R. W. C. and J. A. Jackson (1987). The earthquake of 1980 November 23 in Campania-Basilicata (Southern Italy), *Geophys. J. R. Astr. Soc.* **90,** 375–443.

Institut de Physique du Globe de Strasbourg
5 Rue Rene Descartes
67084 Strasbourg Cedex, France
(H.H., L.R., M.F., A.C.)

Institut de Physique du Globe de Paris
4 Place Jussieu, Tour 14
75230 Paris Cedex 05 France
(R.G., L.M., G.P.)

Osservatorio Geofisico MontePorzio Catonne
Roma, Italy
(R.C., G.G.)

Osservatorio Sismico 'A. Bina'
Perugia, Italy
(M.S.)

Manuscript received 14 July 1988